Rare sugar D-allose induces specific up-regulation of TXNIP and subsequent G1 cell cycle arrest in hepatocellular carcinoma cells by stabilization of p27^{kip1}

FUMINORI YAMAGUCHI[1], MAKI TAKATA[1,3], KAZUYO KAMITORI[4], MACHIKO NONAKA[4], YOUYI DONG[1], LI SUI[4] and MASAAKI TOKUDA[1,2]

[1]Department of Cell Physiology, Faculty of Medicine, and [2]The Rare Sugars Research Center, Kagawa University, 1750-1 Miki-cho, Kita-gun, Kagawa 761-0793; [3]Teikoku Seiyaku Co. Ltd, 567 Sanbonmatsu, Higashikagawa, Kagawa 769-2695; [4]Kagawa Industry Support Foundation, 2217-15 Hayashi-cho, Takamatsu, Kagawa 761-0301, Japan

Received August 21, 2007; Accepted October 18, 2007

Abstract. 'Rare sugars' are defined as monosaccharides that exist in nature but are only present in limited quantities. The development of mass production method of rare sugars revealed some interesting physiological effects of these on animal cells, but the mechanisms have not been well studied. We examined the effect of D-allose on the proliferation of cancer cells and the underlying molecular mechanism of the action. The HuH-7 hepatocellular carcinoma cells were treated with various monosaccharides for 48 h and D-allose was shown to inhibit cell growth by 40% in a dose-dependent manner. D-allose induced G1 cell cycle arrest but not apoptosis. The microarray analysis revealed that D-allose significantly up-regulated thioredoxin interacting protein (TXNIP) gene expression, which is often suppressed in tumor cells and Western blot analysis confirmed its increase at protein level. The overexpression of TXNIP also induced G1 cell cycle arrest. Analysis of cell cycle regulatory genes showed p27^{kip1}, a key regulator of G1/S cell cycle transition, to be increased at the protein but not the transcriptional level. Protein interaction between TXNIP and jab1, and p27^{kip1} and jab1, was observed, suggesting stabilization of p27^{kip1} protein by the competitive inhibition of jab1-mediated nuclear export of p27^{kip1} by TXNIP. In addition, increased interaction and nuclear localization of TXNIP and p27^{kip1} were apparent after D-allose treatment. Our findings surprisingly suggest that D-allose, a simple monosaccharide, may act as a novel anticancer agent via unique TXNIP induction and p27^{kip1} protein stabilization.

Correspondence to: Dr Masaaki Tokuda, Department of Cell Physiology, Faculty of Medicine, Kagawa University, 1750-1, Ikenobe, Miki-cho, Kita-gun, Kagawa 761-0793, Japan
E-mail: tokuda@med.kagawa-u.ac.jp

Key words: D-allose, rare sugar, cell cycle, TXNIP, p27^{kip1}

Introduction

'Rare sugars' are defined as monosaccharides that exist in nature but are only present in limited quantities. There are more than 50 kinds of rare sugars while naturally abundant monosaccharides such as D-glucose and D-fructose are very few in number. Recently, Izumori *et al* developed a simple method to convert D-fructose to D-psicose by D-tagatose 3-epimerase and D-psicose to D-allose by L-rhamnose isomerase (Fig. 1A), facilitating studies of the effects of these rare sugars in animals (1). Among the rare sugars, D-psicose and D-allose showed strong scavenging activity toward reactive oxygen species compared with D-glucose and D-fructose, and D-allose inhibited the production of reactive oxygen from neutrophils (2). D-allose also improved the microcirculation on hepatic ischemia reperfusion (3). Sui *et al* reported that D-allose inhibited the proliferation of some cancer cell lines (4,5), but the underlying mechanisms have remained completely unknown. In this study, we showed that D-allose inhibited cancer cell growth specifically without affecting normal cells and revealed the detail of its molecular mechanism of action via the TXNIP induction.

Materials and methods

Materials. Sugars used in this study including D-glucose, D-fructose, D-psicose, D-allose, D-altrose, D-galactose, D-gulose and D-mannose were supplied by The Rare Sugars Research Center, Kagawa University, Kagawa, Japan.

Cell culture. Human hepatocellular carcinoma (HuH-7) cell line was purchased from the Japanese Cancer Research Resources Bank and maintained at 37˚C under a humidified atmosphere of 5% CO_2 in DMEM (Sigma) supplemented with 10% (v/v) fetal bovine serum and 1% penicillin-streptomycin (GE Healthcare). Normal rat hepatocytes were purchased from the Cell Applications Inc. (San Diego, CA). Cells were maintained on the collagen coated dish in the rat hepatocyte maintenance medium (provided with the kit).

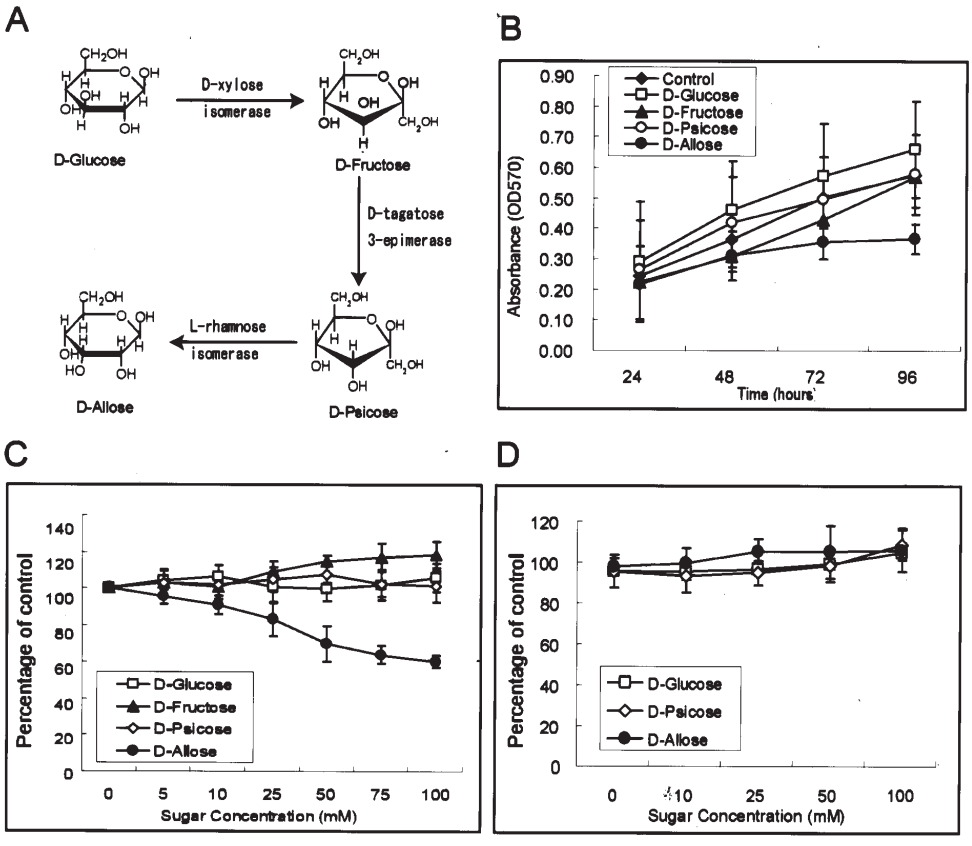

Figure 1. Structures of rare sugars and their effects on the cell growth. (A) D-psicose was converted from D-fructose by the D-tagatose 3-epimerase and further treatment of D-psicose with the L-rhamnose isomerase produced D-allose. (B) HuH-7 cells were treated with 50 mM of various sugars and cell growth was measured by the MTT method. Data shown are mean ± SD values (n=3-4). (C) Various concentrations of sugars were added and cell growth was measured by the MTT method after 48 h. Data shown are mean ± SD values (n=6-11). (D) Normal rat primary hepatocytes were treated with 50 mM of sugars for 48 h and cell growth was measured by the MTT method. Data are mean ± SD values (n=3).

Construction of expression vector and transfection. The full-length human TXNIP, $p27^{kip1}$ and jab1 cDNA were amplified from normal human liver total RNA (Clontech) using specific primers. The TXNIP cDNA was subcloned into pAcGFP1-N1 (Clontech) or pME18s-FLAG mammalian expression vector (6). The human $p27^{kip1}$ cDNA was subcloned into pCMV-Myc mammalian expression vector (Clontech) and jab1 cDNA was subcloned into pEF4/V5-His mammalian expression vector (Invitrogen), and confirmed by sequencing. Constructs were transfected into the HuH-7 cells with Fugene-6 transfection reagent (Roche) following the manufacturer's protocol.

Cell growth assay. HuH-7 cells were grown in 96-well plates at 7,500 cells/well in 0.1 ml medium and cultured for 24 h. Sugars were added to the medium and the cells were further cultured up to 96 h. Proliferation was measured using the 3-(4,5-dimethyl-thiazol-2-yl)-2, 5-diphenyltetrazolium bromide (MTT) method and relative cell growth was expressed as a percentage of the value for untreated control cultures. For the normal rat hepatocytes assay, 96-well plates were coated with a rat collagen and 30,000 cells/well were seeded. The cells were cultured for 24 h and various concentrations of D-allose, D-psicose, or D-glucose were added to the medium. The cells were further cultured for 48 h and processed for MTT assay.

Cell cycle analysis. Cells were cultured with D-allose and harvested by trypsinization, washed twice with ice-cold PBS and fixed in 70% ethanol for 2 h at 4˚C. After washing with PBS and incubation in PBS containing 50 μg/ml propidium iodide (Wako) and 200 μg/ml RNAse A (Sigma) for 30 min, flow cytometric analysis was preformed with a FACSEpics XL flow cytometer (Beckman Coulter). To examine the effect of TXNIP overexpression, cells were transfected with the human TXNIP cDNA cloned into the pAcGFP1-N1 expression vector (Clontech) using the Fugene-6 transfection reagent (Roche). Only transfected cells were sorted and processed for analysis. Effects on the cell cycle were determined with reference to changes in the percentage cell distribution in each phase of the cell cycle and analyzed using System II software (Beckman Coulter). As a control, the expression vector without TXNIP cDNA was used.

cDNA microarray analysis. Total RNA was isolated from HuH-7 cells treated with or without 50 mM D-allose for 48 h using RNeasy mini kit (Qiagen). Five microgram of each sample was converted to cRNA and labeled with Cyanine 5- or Cyanine 3-CTP using Agilent low linear amplification kit. Each probe was denatured and hybridized to the Agilent human oligo microarray for 17 h at 65˚C. The array was washed with 6X SSPE, 0.005% N-Lauroylsarcosine for 1 min,

then 0.06X SSPE, 0.005% N-Lauroylsarcosine for 1 min at room temperature. The array was immersed into the Agilent Stabilization and Drying Solution for 30 sec and dried. The fluorescent signal was scanned using the Agilent microarray scanner and the intensity of signal was analyzed by the feature extraction software (Agilent). The experiment was replicated using different set of samples and data were analyzed with the NIA array analysis software (7). The statistical significance was determined using ANOVA with the False Discovery Rate (FDR) method (P<0.05) proposed by Benjamini and Hochberg (8). Genes were classified using the Database for Annotation, Visualization and Integration Discovery (DAVID 2.1) (9).

Real-time quantitative PCR. The HuH-7 cells were cultured in 24-well plates and 50 mM of various sugars were added to the medium and further incubated. Total RNA was purified and used to synthesize cDNAs with random hexamers. Real-time quantitative PCR was carried out using a Taqman gene expression assay primers and the 7300 real-time PCR system (Applied Biosystems). Each reaction was performed in duplicate. The ß-actin gene was used to normalize across assay and runs and the threshold value (Ct) for each sample was used to determine the expression level of the gene.

Western blotting and immunoprecipitation analysis. After sugar treatment, cells were scraped into a lysis buffer (20 mM Tris-HCl, pH 7.5, 150 mM NaCl, 5 mM EDTA, 0.5% Triton-X-100, 0.5% NP40) with protease inhibitors and treated with sonication. Samples were centrifuged for 10 min at 14,000 rpm and the supernatant was collected. For Western blot analysis, proteins were separated in 10% SDS-PAGE gels, transferred to nitrocellulose membranes blocked with 5% (w/v) non-fat dried milk in TTBS and incubated with anti-flag (Sigma), anti-myc and anti-V5 (Invitrogen), anti-TXNIP, anti-$p27^{kip1}$, anti-$p21^{waf1/cip1}$, anti-p53, anti-Cdk2, anti-Cdk4, anti-cyclin D1, and anti-cyclin E (MBL), or anti-ß-actin antibodies (Sigma). Membranes were probed with a horseradish peroxidase-conjugated anti-rabbit or anti-mouse IgG (Amersham), and signals were detected with an enhanced chemiluminescence system (Amersham). For immunoprecipitation analysis, proteins were incubated with anti-FLAG M2 agarose (Sigma), anti-V5 agarose (Invitrogen) or anti-myc agarose (Invitrogen) and incubated for 2 h at 4˚C. Samples were washed with 0.1% Triton X-100 in TBS and subjected to Western blot analysis.

Immunohistochemistry. Cells were cultured on glass slides and transfected with flag-TXNIP and myc-$p27^{kip1}$ plasmid. After transfection, these cells were further cultured with or without 50 mM D-allose. They were fixed in 4% paraformaldehyde in PBS for 30 min before treatment with cold acetone/methanol for 2 min and blocking with a blocking buffer (3% BSA, 3% goat serum, and 0.1% TritonX-100 in PBS) for 1 h at room temperature. Samples were then incubated with anti-TXNIP or with anti-$p27^{kip1}$ antibodies overnight at 4˚C, then with Alexa Flour 488 or Alexa Flour 594 antibodies (Molecular Probes) for 1 h. Signals were observed under an LSM-GB200 confocal laser scanning microscope (Olympus).

Results

Cell growth assay. The effect of rare sugars on HuH-7 cell growth was assayed by the MTT method. D-glucose, D-fructose and D-psicose did not show any growth inhibitory effects compared with control (no sugar addition), but D-allose significantly suppressed cell growth after 96 h (n=3-4) (Fig. 1B). This effect was dose-dependent and was observed from 5 mM (n=6-11) (Fig. 1C). Rat hepatic primary culture cells were also treated with D-glucose, D-psicose or D-allose to examine whether the growth inhibition by D-allose is specific to the cancer cell line. No growth inhibitory or cytotoxic effects were observed in the normal cells up to 100 mM of sugars tested (Fig. 1D).

Cell cycle analysis. Cells were cultured with or without 50 mM D-allose for 96 h, were harvested and nuclei were stained with propidium iodide. The percentage of cells in each cell cycle phase was analyzed with flow cytometry (Fig. 2A). Without D-allose treatment, 59.0±1.1% of cells were in G1 phase and D-allose significantly increased this to 63.7±1.1% ($p<0.05$, n=4 each). The percentage in S phase decreased from 28.1±1.2% without D-allose to 24.6±1.3% (n=4 each) with D-allose treatment. These observations suggested that D-allose inhibits the HuH-7 cell growth by inducing the G1 cell cycle arrest.

Western blot analysis of cell cycle regulatory proteins. The expression of cell cycle regulatory proteins was analyzed by Western blot after 48 and 96 h of D-allose treatment. The level of cyclin D1, cyclin E and Cdk4 was not changed, whereas the expression of Cdk2 increased after 48 and 96 h of D-allose treatment (Fig. 2B). The expression of $p21^{waf1/cip1}$ and p53 also showed no clear alteration. The level of the $p27^{kip1}$ protein was increased after 96 h both in the presence and absence of D-allose and the extent of the increase with D-allose was significantly greater than without treatment.

Gene expression analysis. The gene expression profiles of HuH-7 cells with or without D-allose treatment was compared by a microarray technique. Approximately 20,000 human genes were analyzed. The experiment was replicated using different set of samples and the statistical significance was determined using ANOVA with the False Discovery Rate (FDR) method (P<0.05). Genes showing >3-fold changes were listed and these genes were classified using the Database for Annotation, Visualization and Integration Discovery (DAVID 2.1) in Table I. There were 37 up-regulated and 11 down-regulated genes observed. Among the up-regulated genes, the expression of the TXNIP was most significantly increased >10-fold). This gene has not been functionally classified, but was reported as a tumor suppressor (10) or metastasis suppressor gene (11). Regarding the cell cycle regulation, the expression of cyclin-dependent kinase inhibitor 2B (CDKN2B) was increased, whereas FK506 binding protein 12-rapamycin associated protein 1 (FRAP1) was decreased. For the transcriptional regulation, homeobox B8 (HOXB8), paired box protein (PAX2) and T-cell acute lymphocytic leukemia 1 (TAL1) was up-regulated and glial cells missing homolog 1 (GCM1) and cofactor

Table I. Gene expression profile of HuH-7 cells after D-allose treatment.

Accession no.	Gene name	Fold change
Unknown		
NM_006472	Thioredoxin interacting protein (TXNIP)	10.5
Cell cycle		
NM_004936	Cyclin-dependent kinase inhibitor 2B (pl5, inhibits CDK4) (CDKN2B), transcript variant 1	3.95
NM_004958	FK506 binding protein 12-rapamycin associated protein 1 (FRAP1)	-3.04
Transcriptional regulation		
NM_003189	T-cell acute lymphocytic leukemia 1 (TALI)	3.01
NM_003643	Glial cells missing homolog 1 (*Drosophila*) (GCM1)	-3.29
NM_004830	Cofactor required for Spl transcriptional activation, subunit 3, 130 kDa (CRSP3), transcript variant 1	-3.27
L25597	Paired box protein mRNA, complete cds	
NM_024016	Homeobox B8 (HOXB8)	4.22
Signal transducer activity		
NM_033179	Olfactory receptor, family 51, subfamily B, member 4 (OR51B4)	3.05
NM_001048	Somatostatin (SST)	3.24
NM_172234	Interleukin 17 receptor B (IL17RB), transcript variant 2	-3.63
NM_001001923	Olfactory receptor, family 5, subfamily C, member 1 (OR5C1)	3.09
NM_004054	Complement component 3a receptor 1 (C3AR1)	-3.37
NM_000684	Adrenergic, ß-1-, receptor (ADRB1)	3.02
NM_144720	Janus kinase and microtubule interacting protein 1 (JAKMIP1)	3.14
NM_005586	MyoD family inhibitor (MDFI)	3.05
NM_021186	Zona pellucida glycoprotein 4 (ZP4)	3.12
Transporter activity		
NM_001045	Solute carrier family 6 (neurotransmitter transporter, serotonin), member 4 (SLC6A4)	-3.13
NM_012283	Potassium voltage-gated channel, subfamily G, member 2 (KCNG2)	3.39
NM_003044	Solute carrier family 6 (neurotransmitter transporter, betaine/GABA), member 12 (SLC6A12)	3.92
NM_001170	Aquaporin 7 (AQP7)	3.01
NM_006514	Sodium channel, voltage-gated, type X, α (SCN10A)	3.55
Ion binding		
NM_019855	Calcium binding protein 5 (CABP5)	3.06
NM_178125	Tripartite motif-containing 50 (TRIM50)	3.12
NM_033386	MICAL-like 1 (MICAL-L1)	3.34
NM_199293	Tyrosine hydroxylase (TH), transcript variant 3	3.64
NM_014677	Regulating synaptic membrane exocytosis 2 (RIMS2)	3.82
NM_207660	Zinc finger CCCH-type containing 14 (ZC3H14), transcript variant 2	-4.23
Nucleotide binding		
NM_002688	Septin 5 (SEPT5)	3.04
NM_007054	Kinesin family member 3A (KIF3A)	-3.11
NM_144583	ATPase, H+ transporting, lysosomal 42 kDa, VI subunit C2 (ATP6V1C2), transcript variant 2	3.55
Catalytic activity		
NM_007180	Trehalase (brush-border membrane glycoprotein) (TREH)	3.48
NM_032385	Chromosome 5 open reading frame 4 (C5orf4), transcript variant 2	3.33
NM_018245	Oxoglutarate dehydrogenase-like (OGDHL)	3.19

Table I. Continued.

Accession no.	Gene name	Fold change
NM_001040	Sex hormone-binding globulin (SHBG)	-3.79
NM_006033	Lipase, endothelial (LIPG)	-3.87
Structural molecule activity		
NM_000394	Crystalin, α A (CRYAA)	3.20
NM_015719	Collagen, type V, α 3 (COL5A3)	3.28
Others		
NM_033377	Chorionic gonadotropin, ß polypeptide 1 (CGB1)	3.81
NM_001012276	PRAME family member 8 (PRAMEF8)	3.58
NM_016651	Dapper, antagonist of ß-catenin, homolog 1 (DACT1)	3.07
NM_001882	Corticotropin releasing hormone binding protein (CRHBP)	3.45
NM_012288	Translocation associated membrane protein 2 (TRAM2)	3.11
NM_203376	Transmembrane protein 81 (TMEM81)	3.48
NM_013364	Paraneoplastic antigen MA3 (PNMA3)	3.05
NM_024770	Methyltransferase like 8 (METTL8)	-3.67
NM_012109	Chromosome 19 open reading frame 4 (C19orf4)	3.14
NM_145172	WD repeat domain 63 (WDR63)	3.32
NM_001012361	WD repeat domain 31 (WDR31), transcript variant 1	3.69

Values are ratios of gene expression levels from D-allose treated cells over control. Microarray experiments were replicated using different sets of samples and the statisticals significance of data was analysed using Anova with the Benjamin and Hochberg False Discovery Rate (FDR) method (P<0.05). Genes up- or down-regulated more than 3-fold were listed and classified using the Database for Annotation, Visualization and Integration Discovery (DAVID 21.1). Genes classified in an ontology group containing a few genes are not listed.

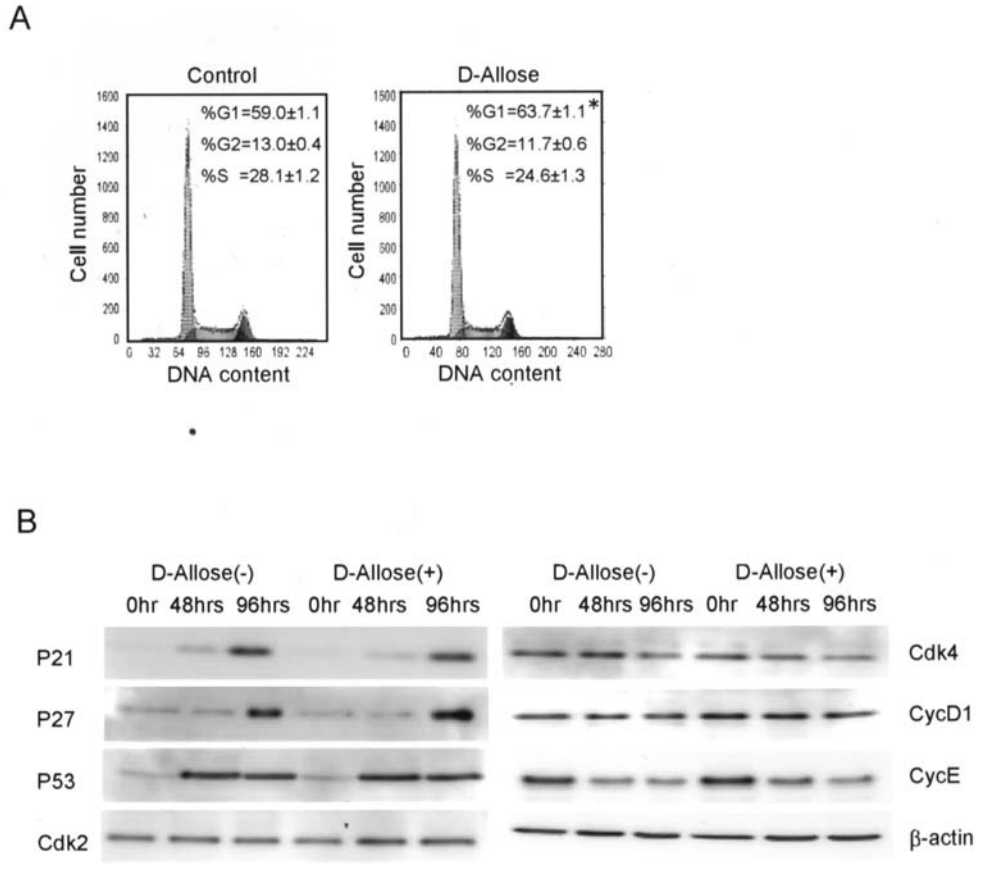

Figure 2. Cell cycle analysis of the HuH-7 cells with or without D-allose. (A) Cells were cultured with or without 50 mM D-allose for 96 h and analyzed by flow cytometry. Data are mean ± SD values. *P<0.05 by Fisher's PLSD analysis (n=4). (B) Western blot analysis of cell cycle regulatory proteins. 0, 48 and 96 h samples with or without 50 mM D-allose treatment were separated by SDS-PAGE and Western blotting was performed with the indicated antibodies.

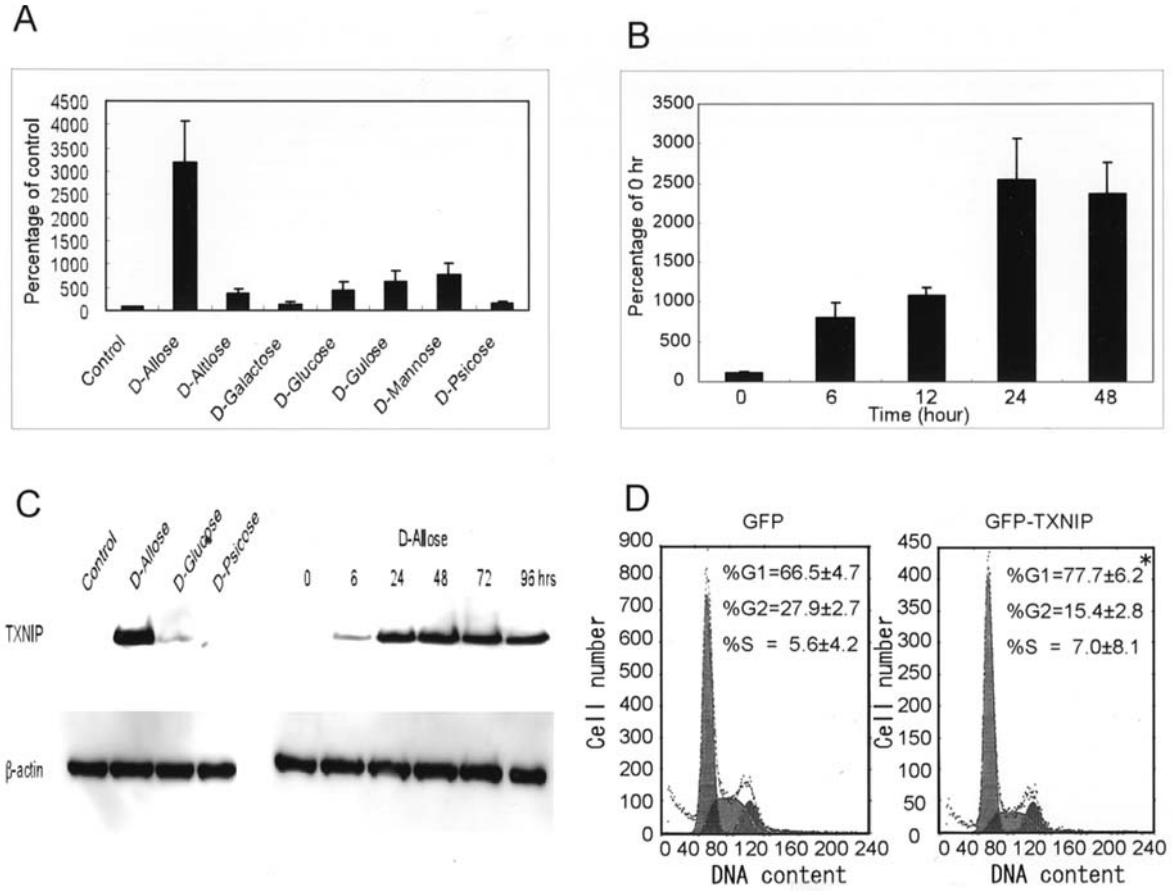

Figure 3. TXNIP induction by various sugars and its association with cell cycle arrest. (A) HuH-7 cells were treated with 50 mM of each sugar for 48 h. Total RNA was extracted and used for real-time PCR. Data are mean ± SD values (n=4). (B) Time course analysis of TXNIP mRNA expression after 50 mM D-allose treatment. Data are mean ± SD values (n=3-6). (C) Western blot analysis of TXNIP. Left panel, sugars were added to the medium of HuH-7 cells and cells were incubated for 48 h. Total proteins were used for Western blot analysis. Right panel, time course of TXNIP protein levels assessed by Western blot analysis. (D) Cell cycle analysis of GFP (as control) or GFP-TXNIP overexpressing HuH-7 cells. Cells were transfected with GFP or GFP-TXNIP expression vector and only transfected cells were sorted and analyzed by flow cytometry. Data are mean ± SD values. *P<0.05 by Fisher's PLSD analysis (n=5).

required for Sp1 transcriptional activation, subunit 3, 130 kDa (CRSP3), transcript variant 1 were down-regulated. D-allose treatment also regulated other genes (5 genes in transporter activity, 9 genes in signal transducer activity, 6 genes in ion binding, 3 genes in nucleotide binding, 5 genes in catalytic activity and 2 genes in structural molecule activity). Eight genes were not classified.

Real-time PCR and Western blot analysis of TXNIP. Based on the result of the microarray analysis, we evaluated the expression of TXNIP by real-time PCR. Various sugars were applied to the HuH-7 cells and cells were incubated for 48 h and the levels of TXNIP induction was compared (Fig. 3A). The D-allose treatment markedly elevated TXNIP expression about 30-fold, although some other sugars including D-mannose, D-gulose and D-glucose also showed a several-fold induction (n=4). The induction of TXNIP by D-allose was already observed after 6 h (n=3-6) (Fig. 3B). Protein levels of TXNIP were also studied by Western blot (Fig. 3C). The expression of TXNIP was compared after sugar treatment. TXNIP protein level was significantly increased by D-allose and to a lesser extent by D-glucose treatment (Fig. 3C). The time course of TXNIP protein level after D-allose treatment revealed that the increase of protein was observed after 6 h and kept at high level until 96 h.

Effect of TXNIP overexpression on cell cycle. The effect of TXNIP overexpression in HuH-7 cells was examined by constructing a GFP-TXNIP fusion protein expression vector and transfection into HuH-7 cells. After transfection of GFP-TXNIP or GFP expression vector (control), cells were harvested and nuclei were stained with propidium iodide. The cells were sorted by the fluorescence of GFP protein to collect the transfected cells only and the percentage of cells in each cell cycle phase was analyzed (Fig. 3D). An increase in the percentage of G1 phase cells was observed in the cells expressing GFP-TXNIP protein compared to that of GFP protein [77.7±6.2% and 66.5±4.7%, respectively ($p<0.05$, n=5 each)].

Immunoprecipitation analysis. To study the molecular mechanism of cell cycle regulation by TXNIP induced by D-allose, the interaction of TXNIP and other interacting proteins, $p27^{kip1}$ and jab1, was evaluated. The flag-TXNIP, myc-$p27^{kip1}$ and V5-jab1 plasmid were co-transfected into HuH-7 cells and immunoprecipitation and Western blot analysis were performed. Interactions between TXNIP and jab1, and between $p27^{kip1}$ and jab1 were observed (Fig. 4A). In addition, D-allose enhanced the interaction of TXNIP and $p27^{kip1}$, although absolute amounts of the proteins were not significantly altered (Fig. 4B).

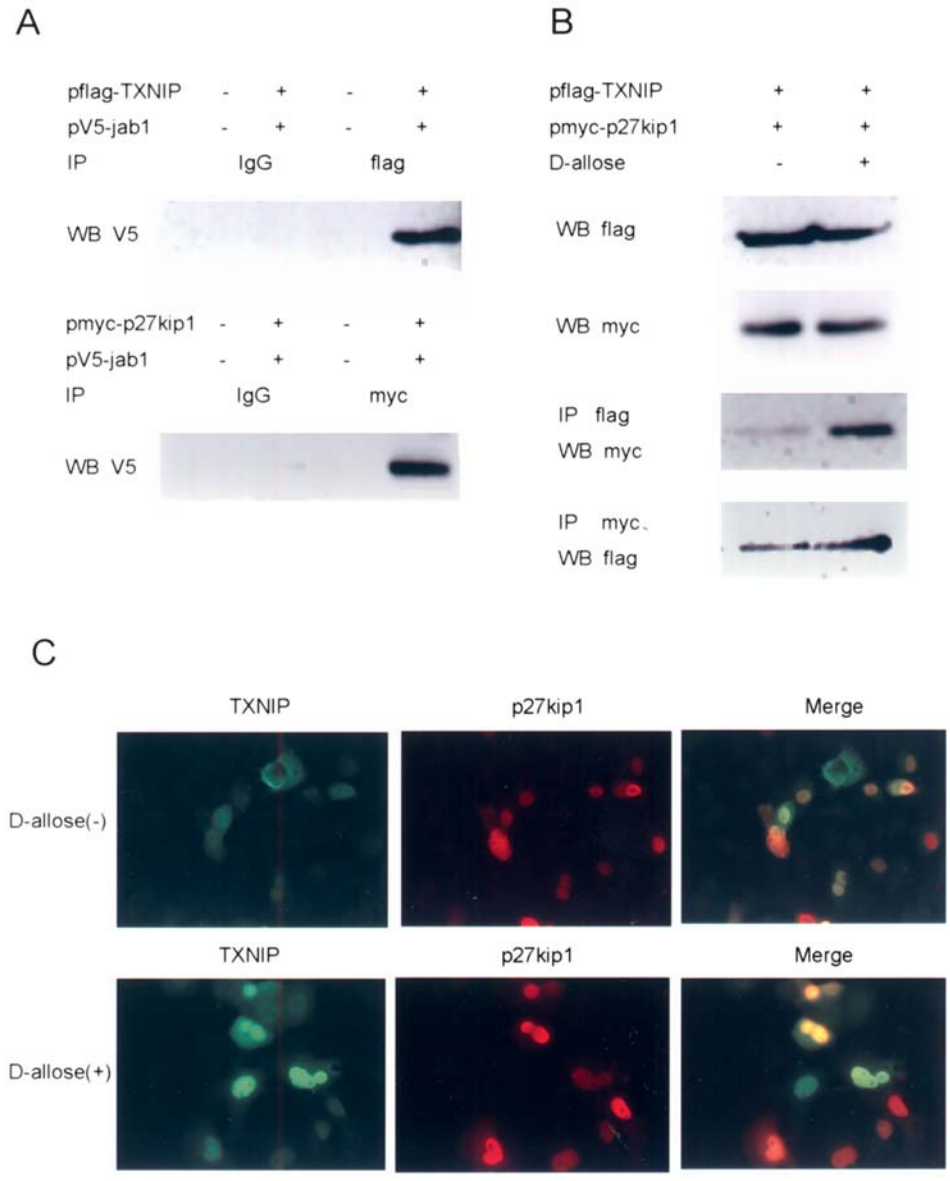

Figure 4. Interaction and localization of TXNIP, $p27^{kip1}$ and jab1 proteins. (A) Flag-tagged TXNIP and V5-tagged jab1 or myc-tagged $p27^{kip1}$ and V5-tagged jab1 plasmid were co-transfected and proteins were immunoprecipitated with either anti-flag or anti-myc agarose. Normal IgG was used as a control. Samples were separated on 10% SDS-PAGE and Western blotting was performed with anti-V5 antibodies. (B) Flag-tagged TXNIP and myc-tagged $p27^{kip1}$ plasmid were co-transfected and cells were cultured with or without 50 mM D-allose for 48 h. Total protein was used for Western blotting with anti-flag or anti-myc antibodies. Immunoprecipitation was also performed with anti-flag or anti-myc agarose, and Western blot analysis was carried out with anti-myc or anti-flag antibodies, respectively. (C) Immunohistochemical analysis of TXNIP and $p27^{kip1}$ with or without D-allose treatment. Flag-tagged TXNIP and myc-tagged $p27^{kip1}$ were cotransfected in HuH-7 cells and treated with or without D-allose. Signal was examined with a confocal laser scanning microscope.

Immunohistochemical analysis. The localization of TXNIP and $p27^{kip1}$ protein was examined by immunohistochemical study. Cells were cultured on glass slides and transfected with TXNIP and $p27^{kip1}$ plasmid before treatment with or without 50 mM D-allose. The localization of these proteins was visualized with anti-TXNIP or with anti-$p27^{kip1}$ antibodies followed by fluorescent antibodies. The result demonstrated that overexpressed TXNIP protein was localized mainly in the cytoplasm without D-allose treatment, while $p27^{kip1}$ was apparent in both the cytoplasm and nucleus (Fig. 4C). However, both proteins were predominantly located in the nucleus after D-allose exposure.

Discussion

The HuH-7 cell growth inhibition was observed by D-allose from 5 mM and is specific to the cancer cells as there was no growth inhibitory or cytotoxic effect on the normal liver cells (Fig. 1D). D-allose inhibited the cell growth by inducing the cell cycle arrest. Compared with the control, D-allose increased the percentage of cells in G1 phase (Fig. 2A). The Western blot analysis showed significant increase of $p27^{kip1}$ protein by D-allose compared to control (Fig. 2B). Cell cycle progression is tightly regulated by regulatory proteins including cyclins, cyclin-dependent kinases (Cdks) and Cdk inhibitors (12,13). Since $p27^{kip1}$ is a key regulator of the

G1 cell cycle progression (14), the result indicated that D-allose causes G1 cell cycle arrest by modulating the level of the $p27^{kip1}$ protein. On the other hand, no apoptotic change by D-allose was observed (data not shown).

To analyze the molecular mechanism in detail, we performed gene expression analysis by the microarray technique. Genes showing >3-fold change are listed in Table I. There were 37 up-regulated and 11 down-regulated genes. Among these, the TXNIP expression was most significantly up-regulated (10.5-fold). This gene was originally cloned as a vitamin D3 up-regulated protein (VDUP1) after 1,25-dihydroxyvitamin D3 treatment of HL-60 cells (15). TXNIP is known to interact with thioredoxin and is involved in the regulation of the redox state of cells (16). This gene is also known as a tumor suppressor (10) or metastasis suppressor (11), and its expression is lower in cancer, including colorectal, gastric and breast cancers, than in normal cells (17,18). This might explain why D-allose inhibits growth of cancer cells effectively without affecting normal cells via TXNIP induction (Fig. 1B and D). In addition, TXNIP-deficient mice show an increased incidence of hepatocellular carcinoma (19), indicating that TXNIP expression is important for the suppression of abnormal cell proliferation such as cancers. In this study, the overexpression of TXNIP caused G1 cell cycle arrest in HuH-7 cells (Fig. 3D). This result supported the idea that the up-regulated TXNIP by D-allose is a key factor for growth inhibition. We compared the TXNIP induction by different sugars and it was more significant by D-allose than other sugars tested (Fig. 3A). The increase of TXNIP was observed after 6 h of D-allose treatment (Fig. 3B and C). There was also slight increase of TXNIP expression by D-mannose, D-gulose, D-glucose and D-altrose. The induction of TXNIP by D-glucose was reported in islet cells (20) or with 2-deoxy-D-glucose and 3-O-methylglucose in the pancreatic beta-cell line INS-1 (21). The mechanism of TXNIP induction by D-allose is not clear, but D-glucose stimulation of TXNIP induction through a carbohydrate response element was reported (20,21). As the structures of D-glucose and D-allose are similar (Fig. 1A), induction by D-allose might be via the similar mechanism, but further investigations are necessary. The microarray analysis showed up-regulation of CDKN2B and down-regulation of FRAP1 (Table I). CDKN2B is one of the CDK inhibitors and controls the G1 cell cycle progression. The FRAP1 has serine/threonine kinase activity and promotes G1 phase progression through signaling to p70/S6 kinase and 4EBP1 (properties of heat and acid stability/eukaryotic initiation factor 4E-binding protein) (22). The increase of CDKN2B and decrease of FRAP1 expression may also contribute the growth inhibitory effect of D-allose.

Regarding the cell cycle regulatory protein, the increase of the $p27^{kip1}$ protein by D-allose was observed without any transcriptional induction (data not shown), indicating possible enhancement of protein stability. Nuclear $p27^{kip1}$ is generally exported to the cytoplasm for ubiquitination and degraded by the 26S proteosome (23). Interestingly, increased rates of proteosome mediated degradation suppress protein levels of $p27^{kip1}$ in cancer cells (24). Nuclear export of $p27^{kip1}$ is known to be mediated by the jab1 (25), originally identified as a co-activator of c-jun and junD (26), incorporated into the COP9 signalosome involved in modulation of gene transcription, signal transduction and protein stability (23). TXNIP is reported to interact with the jab1 competitively and inhibit $p27^{kip1}$ transport, resulting in increased protein levels (27). The immunoprecipitation study confirmed the interaction between TXNIP and jab1, and between $p27^{kip1}$ and jab1 (Fig. 4A). These findings support the work of other research groups (25,27). In addition, we report the first observation of the direct interaction between TXNIP and $p27^{kip1}$ which was significantly enhanced after D-allose treatment (Fig. 4B). The immunohistochemical study showed that overexpressed TXNIP protein was localized mainly in the cytoplasm without D-allose, while $p27^{kip1}$ was apparent in both the cytoplasm and nucleus (Fig. 4C). In contrast, both proteins were predominantly located in the nucleus after D-allose exposure. Together with the immunoprecipitation results, it was suggested that D-allose may cause $p27^{kip1}$ stabilization by restricting the protein to nuclei, possibly through competitive inhibition of the binding of $p27^{kip1}$ and jab1 by TXNIP. In addition, transfer of TXNIP to nuclei would clearly facilitate direct interaction with $p27^{kip1}$ and contribute to its stabilization.

In conclusion, our study generated strong evidence that D-allose may inhibit the growth of cancer cells by specific TXNIP induction and subsequent $p27^{kip1}$ protein stabilization, without exerting appreciable effects on normal cells. D-allose may thus be useful as a novel anticancer drug, providing a new strategy for therapy or prevention in pre-cancerous patients.

Acknowledgements

This work was supported by a research grant from the Cooperative Link of Unique Science and Technology for Economy Revitalization (CLUSTER) Project of Japan.

References

1. Izumori K: Bioproduction strategies for rare hexose sugars. Naturwissenschften 89: 120-24, 2002.
2. Murata A, Sekiya K, Watanabe Y, Yamaguchi F, Hatano N, Izumori K and Tokuda M: A novel inhibitory effect of D-allose on production of reactive oxygen species from neutrophils. J Biosci Bioeng 96: 89-91, 2003.
3. Hossain MA, Wakabayashi H, Izuishi K, Okano K, Yachida S, Tokuda M, Izumori K and Maeta H: Improved microcirculatory effect of D-allose on hepatic ischemia reperfusion following partial hepatectomy in cirrhotic rat liver. J Biosci Bioeng 101: 369-371, 2006.
4. Sui L, Dong Y, Watanabe Y, Yamaguchi F, Hatano N, Izumori K and Tokuda M: Growth inhibitory effect of D-allose on human ovarian carcinoma cells *in vitro*. Anticancer Res 25: 2639-2644, 2005.
5. Sui L, Dong Y, Watanabe Y, Yamaguchi F, Hatano N, Tsukamoto I, Izumori K and Tokuda M: The inhibitory effect and possible mechanisms of D-allose on cancer cell proliferation. Int J Oncol 27: 907-912, 2005.
6. Ishida TK, Tojo T, Aoki T, Kobayashi N, Ohishi T, Watanabe T, Yamamoto T and Inoue J: TRAF5, a novel tumor necrosis factor receptor-associated factor family protein, mediates CD40 signaling. Proc Natl Acad Sci 93: 9437-9442, 1996.
7. Sharov AA, Dudekula DB and Ko MS: A web-based tool for principal component and significance analysis of microarray data. Bioinformatics 21: 2548-2549, 2005.
8. Benjamini Y and Hochberg Y: Controlling the false discovery rate - a practical and powerful approach to multiple testing. J R Stat Soc B 57: 289-300, 1995.
9. Dennis G, Sherman BT, Hosack DA, Yang J, Gao W, Lane HC and Lempicki RA: DAVID: Database for annotation, visualization and integrated discovery. Genome Biol 4: P3, 2003.

10. Han SH, Jeon JH, Ju HR, Jung U, Kim KY, Yoo HS, Lee YH, Song KS, Hwang HM, Na YS, Yang Y, Lee KN and Choi I: VDUP1 up-regulated by TGF-beta1 and 1,25-dihydorxyvitamin D3 inhibits tumor cell growth by blocking cell-cycle progression. Oncogene 22: 4035-4046, 2003.
11. Ohta S, Lai EW, Pang AL, Brouwers FM, Chan WY, Eisenhofer G, Krijger R, Ksinantova L, Breza J, Blazicek P, Kvetnansky R, Wesley RA and Pacak K: Down-regulation of metastasis suppressor genes in malignant phochromocytoma. Int J Cancer 114: 139-153, 2005.
12. Bloom J and Cross FR: Multiple levels of cyclin specificity in cell-cycle control. Nat Rev Mol Cell Biol 8: 149-160, 2007.
13. Malumbres M and Barbacid M: Cell cycle kinases in cancer. Curr Opin Genet Dev 17: 60-65, 2007.
14. Sheer CJ and Roberts JM: CDK inhibitors: positive and negative regulators of G1-phase progression. Genes Dev 13: 1501-1512, 1999.
15. Chen K and De Luca HF: Isolation and characterization of a novel cDNA from HL-60 cells treated with 1,25-dihydroxy-vitamin D-3. Biochim Biophys Acta 1219: 26-32, 1994.
16. Chung JW, Jeon JH, Yoon SR and Choi I: Vitamin D3 up-regulated protein 1 (VDUP1) is a regulator for redox signaling and stress-mediated diseases. J Dermatol 33: 662-669, 2006.
17. Ikarashi M, Takahashi Y, Ishii Y, Nagata T, Asai S and Ishikawa K: Vitamin D3 up-regulated protein 1 (VDUP1) expression in gastrointestinal cancer and its relation to stage of disease. Anticancer Res 22: 4045-4048, 2002.
18. Escrich E, Moral R, García G, Costa I, Sánchez JA and Solanas M: Identification of novel differentially expressed genes by the effect of a high-fat n-6 diet in experimental breast cancer. Mol Carcinog 40: 73-78, 2004.
19. Sheth SS, Bodnar JS, Ghazalpour A, Thipphavong CK, Tsutsumi S, Tward AD, Demant P, Kodama T, Aburatani H and Lusis AJ: Hepatocellular carcinoma in Txnip-deficient mice. Oncogene 25: 3528-3536, 2006.
20. Minn AH, Hafele C and Shalev A: Thioredoxin-interacting protein is stimulated by glucose through a carbohydrate response element and induces ß-cell apoptosis. Endocrinology 146: 2397-2405, 2005.
21. Minn AH, Couto FM and Shalev A: Metabolism-independent sugar effects on gene transcription: The role of 3-O-methyl-glucose. Biochemistry 45: 11047-11051, 2006.
22. Astier AL, Xu R, Svoboda M, Hinds E, Munoz O, Beaumont R, Crean CD, Gabig T and Freedman AS: Temporal gene expression profile of human precursor B leukemia cells induced by adhesion receptor: identification of pathways regulating B-cell survival. Neoplasia 101: 1118-1127, 2003.
23. Tomoda K, Kubota Y, Arata Y, Mori S, Maeda M, Tanaka T, Yoshida M, Yoneda-Kato N and Kato JY: The cytoplasmic shuttling and subsequent degradation of p27kip1 mediated by jab1/CSN5 and the COP9 signalosome complex. J Biol Chem 277: 2302-2310, 2002.
24. Chiarle R, Budel LM, Skolnik J, Frizzera G, Chilosi M, Corato A, Pizzolo G, Magidson J, Montagnoli A, Pagano M, Maes B, De Wolf-Peeters C and Inghirami G: Increased proteasome degradation of cyclin-dependent kinase inhibitor p27 is associated with a decreased overall survival in mantle cell lymphoma. Blood 95: 619-626, 2000.
25. Tomoda K, Kubota Y and Kato J: Degradation of the cyclin-dependent-kinas inhibitor p27kip1 is instigated by jab1. Nature 398: 160-165, 1999.
26. Claret FX, Hibi M, Dhut S, Toda T and Karin M: A new group of conserved co-activators that increase the specificity of AP-1 transcription factors. Nature 383: 453-457, 1996.
27. Jeon JH, Lee KN, Hwang CY, Kwon KS, You KH and Choi I: Tumor suppressor VDUP1 increases p27(kip1) stability by inhibiting JAB1. Cancer Res 65: 4485-4489, 2005.